Extending Boundaries of the Feasible Operations of the Integrated Gas-Electric Systems Using Joint Demand Response Programs

■

Atena Talebi[1], Hossein Sharifzadeh[2*]

■

[1] Department of Electrical Engineering and computer engineering, Hakim Sabzevari University, Sabzevar, Iran
talebia310@gmail.com
[2] Department of Electrical Engineering and computer engineering, Hakim Sabzevari University, Sabzevar, Iran
h.sharifzade@hsu.ac.ir

■

Abstract
While current integrated gas-electric models usually ignore the potentials of demand response programs (DRPs) as an effective operation tool, this paper proposes a novel joint DRP to extend the feasibility of the integrated network operation. Moreover, the presented model considers the practical constraints of compressors and pipelines to construct a more accurate representation of the integrated network compared with the previous models available in the literature. To evaluate the proposed method, a set of scenarios representing a stressed integrated network is considered to simulate the main factors which limit the complete satisfaction of load requirements. The results of the conducted experiments in the considered case study suggest that the joint DRP can extend the boundaries of the feasible regions of the integrated system up to 8%, 28%, and 62% depending on the adopted scenario types. Especially, the simulation results indicate that the proposed model with joint DRP schemes can lead to more optimal solutions than the traditional ones which neglect DRPs.

Keywords: Integrated gas-electric networks, Joint demand response programs, Fuel constraints, Gaspipeline capacity, Extending boundaries of the feasible operations.

* Corresponding author

1. Introduction

Traditionally, power system studies both in planning [1] and operation [2] stages are conducted virtually, independent of other energy systems such as natural gas systems. However, currently, the gas-powered units constitute a large share of demand in gas networks, and it is expected that the share will grow in the future [3]. The reasons behind the trend toward gas-powered units can be explained briefly as follows [4]:

i) They have high efficiency; the efficiency of combined-cycle power plants can reach up to 50%. ii) The gas-fired units can be operated with lower emissions compared with coal-fired power plants. iii) They are fast and flexible. These features are particularly important properties in the current power systems with a high renewable energy penetration. iv) Because of technological advancement, the current natural gas-fired power plants (GFPP) can be constructed with lower investment and time compared with the coal-fired power plants.

Continuously increasing the GFPP share of the total electricity generation, especially in the combine-cycle power plant forms, has challenged the conventional operational planning frameworks of power systems. As the gas-powered units constitute a large share of demands in gas networks, any shortage in gas production or pipeline capacities can affect the security of the power system [5]. For example, in bad weather conditions, gas fuel consumption priority is in the heating sectors rather than the electricity generation; as a result, the gas-powered units may encounter fuel shortages. Therefore, the reliability of the integrated system rather than the individual network has been addressed in recent works [6, 7].

Some studies have focused on the operational challenges of the integrated system. For example, the effects of gas networks on the optimal power flow problems are studied in [8]. To handle the load uncertainties in electric and gas networks, a distributionally robust optimization approach is proposed in [9]. In [10], a probabilistic framework is presented to model different uncertainties in the system. Moreover, the study also considers parameter correlations to model the realistic behavior of the integrated system in a better way. To solve the large-scale problem in multi-energy carrier systems, a decomposing strategy is suggested in [11]. Moreover, Bender's decomposition is presented in [12] to efficiently solve the problem. Integrated operation of the power systems and gas networks considering solar energy systems is studied in [13]. A market-clearing and pricing mechanism for the integrated network incorporating wind generations is analyzed in [14]. In [15], a combined heat and power model with gas turbines is considered while attempting to enhance some reliability criteria. The effects of electric vehicles in the integrated network are analyzed in [16]. A unit commitment model considering transient constraints of gas pipelines is addressed in [17].

The DRP as an effective tool for enhancing the performance of the integrated system is discussed in some recent studies such as [18, 19]. However, its potential to extend the feasible operation boundaries of the integrated network has not been well addressed. Moreover, previous studies solely focus on electric loads, as the DRP tool, and ignore the capability of gas loads to support the integrated system security.

Moreover, from the accuracy point of view, the feasible operating range of compressors [20] and pipeline restrictions [21] are rarely considered in the gas network representation in integrated models. In other words, the considered gas network models in current studies are rather simplistic and may not accurately reflect the practical behavior of the network and its impact on the operation of the integrated system. This may result in a infeasible scheduling of the integrated network.

Therefore, in this paper, a detailed formulation is constructed to capture the integrated network behavior better. Moreover, the effectiveness of the proposed joint DRP is evaluated using a more accurate model.

The contribution of this paper can be summarized as follows:

A) As the main contribution of this paper, a new-joint DRP is proposed to extend the feasible region boundaries of the integrated network. Particularly, as an advantage, the proposed model can lead to more optimal solutions than the traditional ones which neglect DRPs.

B) To identify the feasible regions of the integrated model closely, an exact model of a gas network is employed considering the nonlinear non-convex characteristics of compressors as well as velocity constraints in gas pipelines.

In the next section, firstly the proposed model of the integrated system including the joint DRP scheme is introduced. In the next section, the concept behind our idea to use the joint DRPs for extending the feasible area of the integrated network and, to some extent for improving the efficiency of the systems is clarified. Then, in Section IV, the applications of the proposed model are verified by some designed scenarios which stress the integrated network. The last Section is devoted to the conclusion.

2. Problem Formulation

Here, an integrated model of the gas-electric system with the suggested joint DRPs is presented. To this end, firstly a short-term model for an electric network operation [22] along with the coupling constraints with a gas network is provided. Then, a detailed model representing the gas network elements [23] is introduced, while the coupling constraints with the electric network are also addressed. Fig. 1 displays the general framework of the proposed method elaborated in the following.

2.1. A Generation Scheduling Model in Power Systems

The objective function of a generation scheduling model minimizes the total operation cost that can be expressed as follows:
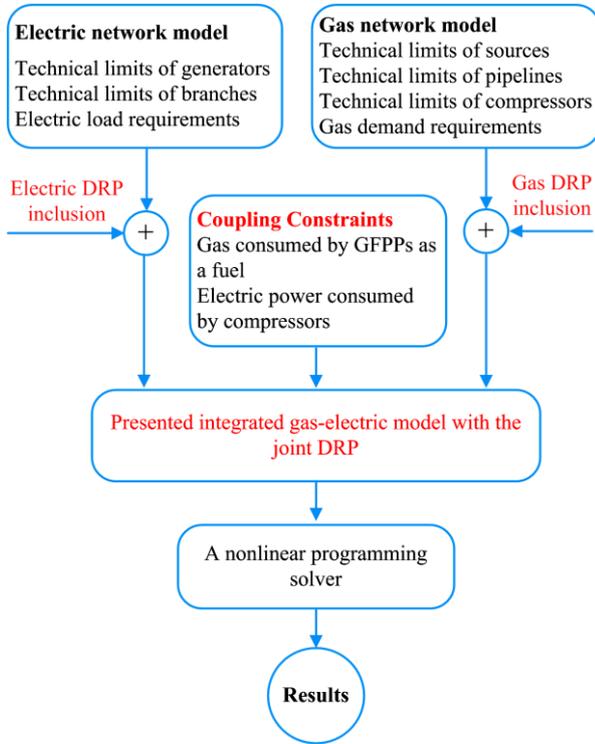

Fig. 1: General framework of the proposed method

$$Minimize \sum_{\forall i \in G_i} k_i P_i + \sum_{\forall i \in G_{GFPP}} \rho_i P_i +$$
$$\sum_{\forall j \in N} \xi_i L_i (1 - D_j^E) + \sum_{\forall v \in V} \psi_v q_v (1 - DR_v^G) \quad (1)$$

The model constraints, stemmed from technical limits of power system elements, are described as below [22]:
- Power generation limits,
$$P_i^{min} \le P_i \le P_i^{max} \quad (2)$$

- Branch capacity constraints,
$$\left| P_{kj} \right| \le P_{kj}^{max}, \forall (k,j) \in C_{Br} \quad (3)$$

- The power balance equation with the DRP option,
$$\sum_{i:(i,j) \in C_G} P_i - \sum_{k:(k,j) \in C_{Tr}} P_{kj} - \sum_{CM:(c,j) \in V_E} E_{CM} =$$
$$L_j \times DR_j^E, DR_j^E \in [0,1], \forall j \in N \quad (4)$$

The term $\sum_{CM:(c,j) \in V_E} E_{CM}$ stands for the electrical power consumed by gas network compressors. The symbol DR_j^E represents the electrical load shedding factor. For example, $DR_1^E = 0$ indicates that an electrical load in bus#1 is completely curtailed.
- DC approximation of branch flows,
$$P_{kj} = \frac{1}{x_{kj}} (\theta_k - \theta_j), \forall (k,j) \in C_{Br} \quad (5)$$

- Gas consumed by the GFPPs,
$$F_i = f_i(P_i), \forall i \in G_{GFPP} \quad (6)$$

Here, a linear relationship between the electrical generation and the GFPP consumed gas is considered.
- Total gas consumption limit for the GFPPs,
$$\sum_{\forall i \in G_{GFPP}} F_i = F_{Total} \quad (7)$$

It is noted that the reactive power also can be taken into account in the formulation using the AC power flow (PF) equation. However, as it was also stated in [24], the current electricity market clearing mechanisms do not consider the AC PF due to its highly nonlinear non-convex nature. As the integrated model is a larger optimization problem that has the constraints of two different networks, the proposed model does not consider the AC PF to present a more tractable model.

2.2. Gas Network Modeling

Natural gas flows in gas pipelines from higher pressure to lower pressure. Similar to power systems, gas networks are composed of distribution and transmission networks with different nominal pressures and mass flows. The compressors in gas networks can control pressure levels. Here, gas sources, sinks (or demand), pipelines, and compressors are modeled to represent gas networks as follows [23]:
- Mass flow conservation constraints,
$$\sum_{s:(s,v) \in C_S} q_s - \sum_{u:(u,v) \in C_{pipe}} q_{uv} - \sum_{i:(i,v) \in I_G} F_i =$$
$$q_v^D \times DR_v^G, DR_G \in [0,1], \forall v \in V \quad (8)$$

The term $\sum\limits_{i:(i,v)\in I_G} F_i$ stands for the amount of gas consumed by the GFPPs. The symbol DR_v^G describes the gas load curtailment factor. For example, $DR_1^G = 0$ implies that the whole gas load in node#1 is curtailed.

- Source flow limits,

$$q_s \leq q_s^{\max}, \forall s \in S \tag{9}$$

- The pressure limits of nodes,

$$p_v^{\min} \leq p_v \leq p_v^{\max}, \forall v \in V \tag{10}$$

-The mass flow limits of pipelines

$$q_{uv}^{\min} \leq q_{vu} \leq q_{uv}^{\max}, \forall (u,v) \in C_{pipe} \tag{11}$$

- The gas velocity constraint: vibrations due to high flow velocity may create noise as well as burst the pipes. Therefore, flow velocity should be limited in the head and tail of the pipes:

$$v_{uv} = \frac{R_s T q_{uv}}{A_u p_u} z_{uv} \leq v_{uv}^{\max}, \forall (u,v) \in C_{pipe} \tag{12}$$

- Pressure loss equation,

$$p_v^2 - p_u^2 = \frac{L_{uv} \lambda_{uv} R_s z_{uv} T}{A_{uv}^2 D_{uv}} \leq |q_{uv}| q_{uv}, \tag{13}$$
$$\forall (u,v) \in C_{pipe}$$

The equation (13) is known as Weymouth Equation. Here, the Papay equation is employed to calculate the compressibility factor z_{uv} as follows:

$$z_{uv} = 1 - 3.52 p_r \exp(-2.26 T_r) + 0.274 p_r^2 + \exp(-1.878 T_r), \forall (u,v) \in C_{pipe} \tag{14}$$

To compute the mean pressure used in the Papey Equation ($p_r = \frac{p_{uv}^m}{p_c}$), the node pressure, lower and upper bounds, are utilized:

$$p_{uv}^m = \frac{1}{2}(\max(p_u^{\min}, p_v^{\min}) + \min(p_u^{\max}, p_v^{\max})) \tag{15}$$
$$\forall (u,v) \in C_{pipe}$$

Moreover, the formula of Nikuradse is employed to obtain the friction factor λ:

$$\lambda_{uv} = (2 \times \log_{10} \frac{D_{uv}}{kr} + 1.138)^{-2} \tag{16}$$

- The maximum and the minimum permissible pressure increase by the compressors,

$$p_{CM,u} - R_{CM}^{\max} p_{CM,v} \leq 0 \tag{17}$$

$$p_{CM,o} - R_{CM}^{\max} p_{CM,in} \leq 0 \tag{18}$$
$$(17),(18): \forall CM \in X, \forall (u,v) \in M_{uv}$$

- Feasible operating range (FOR) of the compressors
The compressor is of particular significance in a gas network as it controls the pressure levels in the network. However, most of the previous studies represent the compressor model as a simple output/input ratio and neglect its practical constraints. The simple model may not capture the practical limitations of the compressor, and, thus, the derived operating point from the corresponding optimization model may violate the feasible operation range of the compressors.

To accurately capture the operating range of the compressor, the characteristic diagram of the compressor should be taken into account. The typical feasible operation range, i.e. its characteristic diagram, of a turbo compressor is depicted in Fig. 2. In the diagram, the horizontal axis usually shows the mass or volumetric flow, and the vertical axis represents the specific change in adiabatic enthalpy or pressure ratio. The characteristic diagram is usually drawn by curve fitting techniques using some recorded measurements. The dashed lines and the solid lines in the figure represent the iso-line for the specific efficiency and speed respectively. The diagram is limited by four curves. The upper and the lower limits of the diagram are established by the minimum and maximum compressor permissible speed. The right area of the diagram is restricted by the so-called stonewall or choking line where gas velocity may reach sonic velocity and hurt the blades and the motors. The surging line limit prevents the compressor from operating in unstable conditions damaging the compressor bearings. In other words, the surge and choking lines show the allowable minimum and maximum flow rate of a compressor.

The diagram builds two pairs of constraints for a compressor feasible operation. The first constraints enforce minimum velocity and the stonewall line in the following form:

$$H_{CM} \geq \sigma_2 Q_{CM}^2 + \sigma_1 Q_{CM} + \sigma_0, \forall CM \in X \tag{19}$$

The maximum velocity and the surge line can be expressed as follows:

$$H_{CM} \leq \rho_2 Q_{CM}^2 + \rho_1 Q_{CM} + \rho_0, \forall CM \in X \tag{20}$$

The operating range of the compressor is a non-convex area challenging optimization solvers. To solve the problem, the area can be approximated by its convex hull as described in [23].

From the accuracy viewpoint, the previous studies in the area generally ignore the practical characteristic of

the compressors. Therefore, their model solutions may violate the FOR of the compressor leading to an infeasible solution probably. The same discussion may be applied to the velocity constraints in gas pipelines.
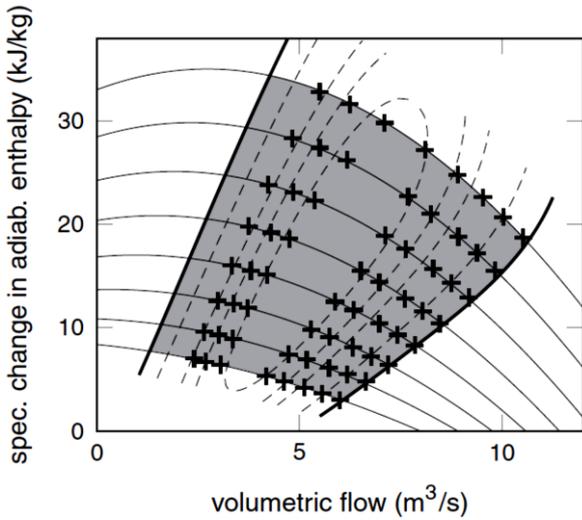

Fig. 2: Characteristic diagram of a compressor [23]

Finally, it is noted that because of the pressure loss equation in (13), the presented framework is a nonlinear model and, thus, should be solved with nonlinear programming techniques.

3. Proposed Method

The change of the philosophy of power system operation from strictly satisfying load requirements to operating the system in the most efficient conditions requires some new strategies and more effective tools. DRPs with considerable flexibility and lower costs compared with enormous capital expenditures of power system expansions have gradually gained acceptance among researchers. On the other side, although penetration of GFPPs poses a challenge to the power system operations, it provides some new resources to increase the flexibility of the integrated network as an advantage.

In this paper, a new combined electrical load/gas curtailment technique is developed to enhance the flexibility of both systems and to widen the feasible region of the integrated network. The concept behind the proposed idea is illustrated in Fig. 3.

A: feasible region of the electric network
B: feasible region of the gas network
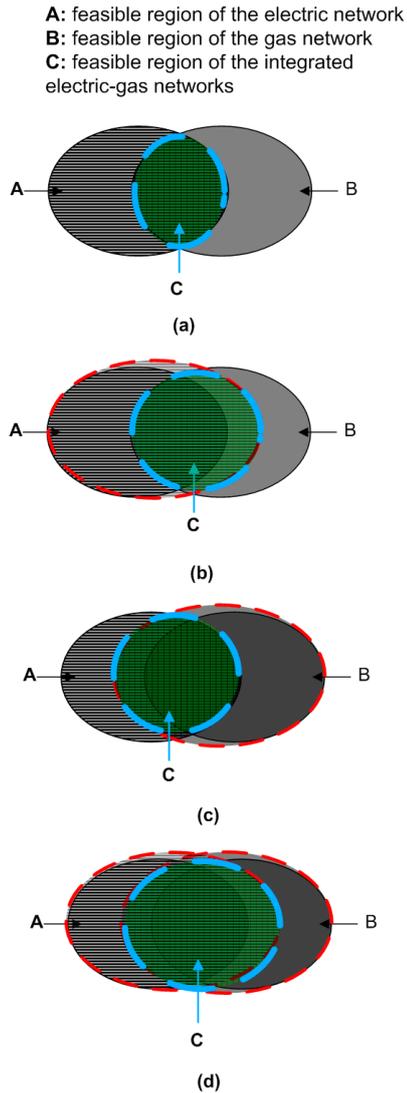**C:** feasible region of the integrated electric-gas networks

Fig. 3: A simplified feasible region representation of the integrated network: (a) without DRP. (b) with the electrical DRP. (c): with the gas DRP. (d) with the joint DRP

The simplistic boundaries of practical operation regions of an integrated system are illustrated in Fig. 3. The joint feasible space of the gas-electric system without the DRP is identified by the intersection of the feasible regions of the electric and the gas systems shown in green Fig.3.a. Taking into account the gas load curtailment and the electric load shedding individually, the combined feasible ranges can be represented with Fig.3.c and Fig.3.b respectively. The regions are illustrated by green sections; they clearly provide wider areas compared with Fig.3.a. Finally, a more extended feasible space of an integrated network can be achieved by the inclusion of both electric load shedding and gas load curtailment. This is depicted in Fig.3.d implying that a wider feasible space may be obtained utilizing the joint DRPs.

In this paper, the achievable extended space of the integrated system, thanks to the joint DRP, is studied.

To the best of our knowledge, this is the first attempt to enhance the flexibility of the integrated network utilizing the joint DRP while accounting for a detailed model of gas network elements.

4. Simulation Results

To study the efficacy of the DRP to extend the boundaries of the feasible operations of the integrated gas-electric systems, the 118-bus power system test case [25] together with a 40-node gas network [26] is considered. The topology of the gas network [27] and the considered GFPPs are shown in Fig. 4. The presented nonlinear model is solved using the IPOPT solver (as a nonlinear solver) within the GAMS software [28]. All simulations are performed on a laptop with a 2.4 GHz Intel Core i3 CPU and 4 GB of RAM. Since a small number of electric/gas loads are generally volunteered to be curtailed in emergency conditions based on their contracts, solely 7 electrical loads and 7 gas loads are considered to be dispatchable among 99 load buses, 29 sink nodes in the 118-bus, and the 40-node systems respectively. The mentioned dispatchable loads are shown in Table 1.

Table. 1: The list of dispatchable loads in the integrated system

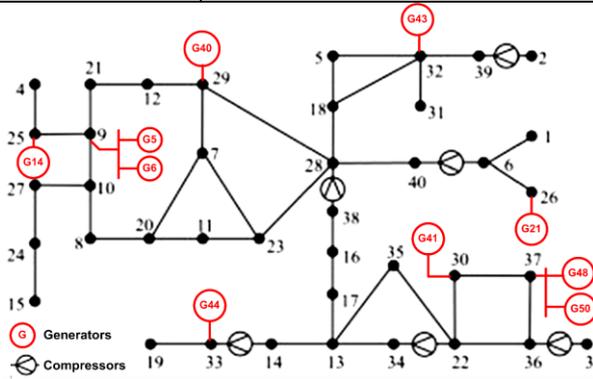| Network	Dispatchable loads
40-nodegas network	u1, u4, u9, u17, u18, u26, u27
118-bus electric network	Bus54, Bus59, Bus75, Bus76, Bus80, Bus90, Bus116

Fig. 4: 40-node gas network and the considered GFPPs

To study the interdependency of the electric and gas networks and also to evaluate the efficacy of the proposed joint DRP to extend the feasible region of the integrated network four different experiments are conducted as follows:

(I) Limitation on consumed gas as the GFPP fuel
(II) Limitation on pipeline capacities
(III) Electrical and gas load increase scenario

Three experiments are presented to show the ability of the joint DRP to enhance the integrated network performance and also to extend the boundaries of the feasible operations of the integrated gas-electric system.

In the following experiments, the parameters α, β and γ change linearly in a fixed step 0.01 and continue until arriving at infeasible solutions.

Experiment (I): Limitations on the consumed gas fuel: The amount of gas consumed by the GFPPs in power systems may be limited due to an agreed contract or other reasons such as extremely cold weather conditions. Here, the effect of the limit on operational decisions is studied directly by introducing a fuel limit factor in constraint (7) as follows:

$$\sum_{s \in S} F_s \le \alpha \times F_{total} \tag{21}$$

Then, parameter α is decreased linearly in a fixed step 0.01 and the obtained results are recorded in each step. The results are illustrated in Fig. 5.

It is noted that in all following figures, the blue lines show the cost, computed using (1), while the green lines represent GFPP generations. Besides, the solid lines correspond to the base case, i.e. without any DRPs, while the dotted lines refer to the results of the proposed joint DRP. The 'Feasible area' denotes the feasible space before the application of the DRP. The 'Extended feasible area' represents the additional feasible space obtained using the joint DRPs. The 'Infeasible area' indicates that no feasible solution can be identified in the area even by the DRPs. The yellow and the red dotted lines demonstrate the feasible boundaries before and after the DRP application respectively. As mentioned earlier, the 'base case' refers to the model without incorporating load curtailment schemes.

Firstly, Fig. 5 shows that as the gas fuel is further restricted, the operation cost is increased considerably. In other words, by limiting gas consumption, GFPP generations are replaced with some more expensive units; as a result, the total operation cost increases. The minimum α, leading to a feasible solution without the load shedding application, is 0.87. Nonetheless, the feasible space can be extended by leveraging the joint DRPs. As it was stated earlier, the dotted lines imply the extension of the feasible solutions using the proposed load curtailment approach beyond the previous boundaries. The yellow and the red dotted lines in the figure reveal that the DRP pushes the feasible boundary so that a wider practical operation range is possible up to α=0.8. This shows an 8% improvement in the feasible boundary ($\frac{0.87 - 0.8}{0.8} \times 100$). Noteworthy, the 'infeasible area' shown in the figure may be further shrunk utilizing more volunteered loads to shed. Nevertheless,

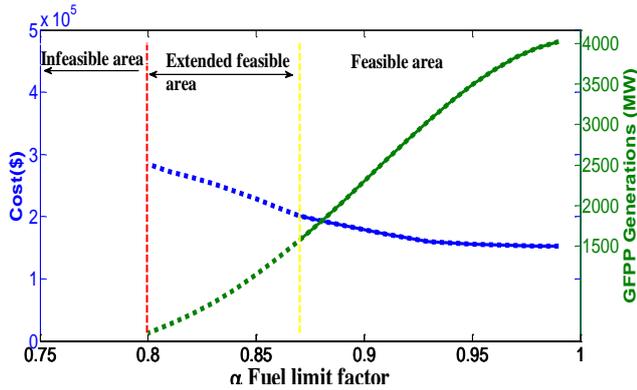in this paper, solely 7 loads can contribute to DRPs as listed in Table 1.

Fig. 5: Effect of the fuel limitations on the operation cost and the GFPP generations

Experiment (II): Limitation on the Pipeline Capacities: Nowadays, gas pipelines play a critical role not only in gas networks but also in power systems, especially the outage of a large pipeline supplying some GFPPs which may cause power system blackout due to shortage in electric generations. A scenario is simulated; in that scenario, the pipeline capacities have been reduced because of some events such as pipeline outages or bad weather conditions. To this end, the pipeline capacities in the case study are decreased by γ as a factor:

$$|q_{uv}| \le \gamma \times q_{uv}^{\max}, \forall (u,v) \in C_{pipe} \tag{22}$$

The total-incurred cost and GFPP generations as the functions of the factor γ are exhibited in Fig. 6. As it can be seen in this figure, the cost increases as the factor reduces, namely as the pipeline capacities decrease. Predictably, GFPP generations also reduce correspondingly. Particularly, in $\gamma = 0.61$, no feasible solution can be obtained in the integrated operation. This cannot be identified in the independent operational planning of the power system and the gas network.
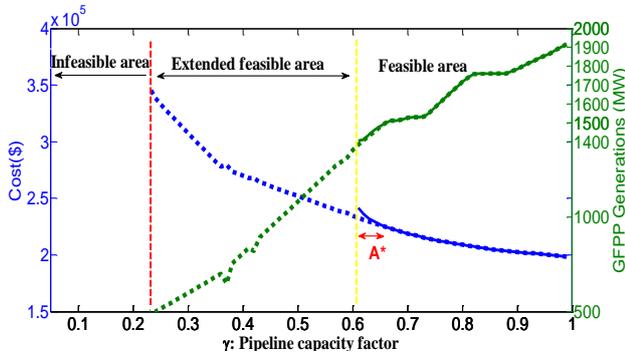

Fig. 6: Effect of the pipeline capacities on the operation cost and the GFPP generations

Utilizing the load curtailment strategy, the feasible limit can be extended up to $\gamma = 0.23$ suggesting a 62%

enhancement ($\frac{0.61 - 0.23}{0.61} \times 100$). Same as the earlier figure, the dotted lines represent the obtained results taken load curtailment into account.

As it is illustrated in this figure, in the initial stages of the pipeline congestion, the proposed model does not deploy load shedding and, thus, the two-cost curves follow the same trajectory exactly. It is probably an expected result as load curtailments usually are considerably more expensive than the generation of power plants. However, a particularly important outcome of the proposed model with the DRP is achieving lower costs compared with the base case (i.e. without load curtailment) even before the base case infeasible line ($\gamma = 0.61$). See the part of the figure shown by A* where the costs of the load curtailment approach lie below the base case costs.

As noted earlier, the viewpoint on energy system operations, especially on power systems, have changed from firmly meeting load requirements to operating the systems most efficiently. Part A* reveals that the new philosophy has been considered in the presented formulation with DRPs. In other words, the model adopts load shedding decisions rather than load satisfaction whenever load curtailments result in a more optimal solution compared with the traditional load fulfilling strategy. To put it simply, the consumers prefer to incur the load curtailment rather than to serve with a huge expenditure.

As an example, the achieved cost, GFPP generation, and load curtailment actions obtained based on the two different viewpoints are presented in Table 2 for $\gamma = 0.61$, i.e. in the infeasible boundary of the base case. The table demonstrates that 'the most economic operation' point of view, which utilizes the joint DRP, leads to a more optimal solution compared with the traditional viewpoint, namely 'meeting load strictly'. As the proposed model includes the load curtailments as the additional control variables compared with the base case, it can optimize the economic performance of the integrated network more efficiently.

Table. 2: Comparison of the obtained results in the two different operation philosophies for the experiment (II)

The operation viewpoint	Cost($)	GFPP generation (MW)	Load curtailment	
			Electric (p.u.)	gas
Meeting load strictly	241754.0	1404.6	0	0
The most economic Operation	232716.9	1382.5	2.41	0

The details of the required electrical load shedding actions for the 'most economic Operation' in $\gamma = 0.61$

are shown in Fig. 7. As stated in Table 2, solely electric load shedding is required at the point. Among the seven-volunteer load buses listed in Table 1, Bus59, Bus75, and Bus76 are selected to curtail in $\gamma = 0.61$.
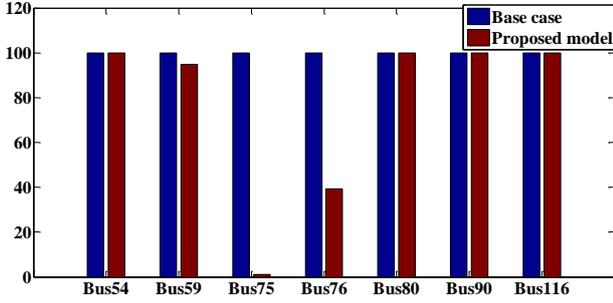

Fig. 7: Optimal electric load curtailment in $\gamma = 0.61$

Experiment (III): Electrical and Gas Load Increase Scenario: In this experiment, both electric and gas networks are stressed directly using a demand increase scenario as follows:

$$\sum_{s:(s,y)\in C_S} q_s - \sum_{u:(u,y)\in C_{pipe}} q_{uv} - \sum_{i:(i,y)\in I_G} F_i =$$
$$\beta \times q_v^D \times DR_v^G, DR_G \in [0,1], \forall v \in V \tag{23}$$

$$\sum_{i:(i,j)\in C_G} P_i - \sum_{k:(k,j)\in C_{Tr}} P_{kj} - \sum_{CM:(c,j)\in V_E} E_{CM}$$
$$= \beta \times L_j \times DR_j^E, DR_j^E \in [0,1], \forall j \in N \tag{24}$$

The changes in the cost as well as GFPP generations are displayed in Fig. 8. As it can be seen in the figure, the demand growth dramatically increases the incurred cost. Moreover, the figure shows that for some β the feasible solution may not be found for the joint operation as also observed in the previous experiments.
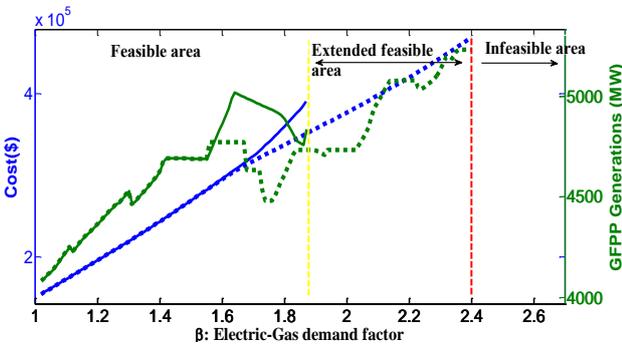

Fig. 8: Effect of the gas demand increase on the operation cost and the GFPP generations

The last feasible point in the base case corresponds to $\beta = 1.87$. However, employing DRPs, the feasible pace can be extended up to $\beta = 2.4$ implying a 28%

improvement ($\frac{2.4 - 1.87}{1.87} \times 100$). Moreover, yet again, the figure shows that the incurred costs can be reduced even before the base case infeasible line ($\beta = 1.87$).

For the sake of conciseness, details pertaining to the load curtailment decisions in the present experiment are not reported.

The cost, GFPP generation, and the required load curtailment actions in two approaches for experiment III are reported in Table 3 for $\beta = 1.87$, i.e. in the infeasible boundary of the base case. As it can be seen, the proposed model with joint DRPs results in a lower cost compared with the base case approach. Moreover, the proposed model presents a lower GFPP generation as it seems economically more optimal;that is, a part of load increases to be compensated with the planned DRP rather than with the generation increase.

Table. 3: Comparison of the obtained results in the two different operation philosophies for the experiment (III)

The operation viewpoint	Cost($)	GFPP generation (MW)	Load curtailment	
			Electric (p.u.)	gas
Meeting load strictly	390792.6	4835.7	0	0
Most economic Operation	350973.6	4734.2	23.151	0

As mentioned earlier, the parameters α, β and γ change linearly in a fixed step 0.01. The changes continue until arriving at an infeasible solution. Thus, the number of steps (or distance to infeasibility) to arrive at the infeasible line is considered as a criterion for improving the feasible space. Using the criterion, individual and joint contributions of the electric and gas load curtailments to the extension of the feasible space of the integrated networks are displayed in Fig. 9.

As it can be seen in the figure:

1) The joint gas-electric load curtailment is the most effective approach when the integrated system comes across the pipeline congestions.

2) The electric load shedding seems a more effective tool to extend the feasible space than the gas load curtailment in all conducted experiments.

3) The smallest feasible space for the integrated system pertains to the experiment (I), i.e. when the system encounters gas fuel limitations.
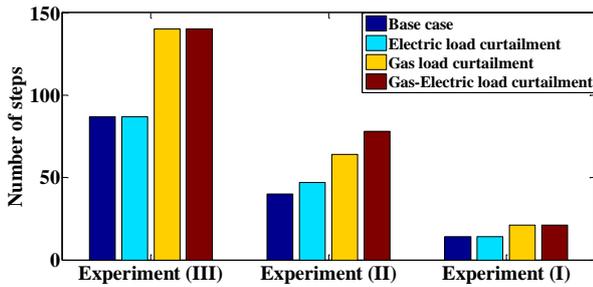
Fig. 9: Efficacy of the individual and joint DRP on the extending boundaries of the feasible operations

5. Conclusion

In this paper, a new formulation is presented modeling both grid characteristics more precisely, especially the compressor representation details, thereby it enhances the ability of the model to simulate the integrated system operation more realistically. To study the network interactions and, especially to evaluate the proposed joint DRP efficacy, three different experiments are conducted to stress the integrated network. Firstly, as the obtained results show, the designed experiments including the fuel limitations, the pipeline capacity congestion, and the electric-gas demand increase may highly influence the variables of the power system operation and result in infeasibility-- i.e. the impractical operational decisions in extreme conditions. Secondly, as the simulation results revealed, the largest practical operation ranges-- i.e. the feasible space-- are achievable utilizing the joint electric-gas load curtailment rather than the individual gas or electric load shedding. Apart from the feasible space extension, the presented joint DRP approach agrees with the new philosophy of energy system operations, namely the most efficient operation rather than meeting load strictly. As a result, as an advantage, it usually leads to more optimal solutions than the traditional strategy.

Nomenclatures

Indices

CM	Index of gas compressor
i	Index of generator
k, j	Index of a power system bus
m	Index of a gas pipeline
s	Index of a gas source
u, v	Index of a gas network node

Sets

C_s	Incidence matrix of nodes and gas sources
C_G	Incidence matrix of buses and generators
C_{Br}	Set of branches
C_{Pipe}	Set of gas pipelines
G_i	Set of non-gas powered generators
G_{GFPP}	Set of gas-powered generators
I	Set of generators
I_G	Incidence matrix of GFPPs and nodes
M_{uv}	Set of arcs with compressors
N	Set of buses
S	Set of gas sources
V	Set of gas network nodes
V_E	Incidence matrix of compressors and buses
X	Set of gas compressors

Parameters

A_{uv}	Pipeline cross-section area
F_{Total}	The upper bound for gas consumption in GFPP
kr	Roughness
L_{uv}	Pipeline length
L_j	Bus load
p_c	Pseudocritical pressure
p_{uv}^m	Average pressure
p_r	Reduced pressure
$P_i^{\min}$, $P_i^{\max}$	The minimum and maximum permissible active power output of generators
$p_v^{\min}$, $p_v^{\max}$	Node minimum and maximum permissible pressure
$q_{uv}^{\min}$, $q_{uv}^{\max}$	The minimum and maximum permissible flow at pipeline uv
q_v^D	Node gas demand
$q_s^{\max}$	Upper bound for the flow of gas source
R_s	Specific gas constant
$R_{CM}^{\min}$, $R_{CM}^{\max}$	The minimum and maximum pressure ratio of the compressor
T	Gas temperature
T_r	Reduced temperature
T_c	Pseudocritical temperature
$v_{uv}^{\max}$	Gas velocity
x_{kj}	Branch reactance
z_{uv}	Compressibility factor
λ_{uv}	Friction factor
$\sigma_2, \sigma_1, \sigma_0,$ ρ_2, ρ_1, ρ_0	Coefficients of compressor characteristic
κ_i , ρ_i	Cost coefficient of non-gas and gas-powered generators respectively
ζ_j, ψ_v	Electric and gas load curtailment costs respectively

Variables

DR_j^E	Electric demand response factor
DR_v^G	Gas demand response factor
E_{CM}	Electrical power consumed by the compressor
F_i	Consumed gas by GFPP
H_{CM}	Specific change in adiabatic enthalpy
$P_{CM,O}$, $P_{CM,in}$	Output and input pressure of the compressor
P_i	Generation level

P_{kj}	Branch flow	q_{uv}	Pipeline flow
p_v	Node pressure	v_{uv}	Gas velocity
Q_{CM}	Compressor volumetric flow	θ_k	Voltage angle
q_S	Gas source flow		

References

[1] Mohseni, A., Abedi, M. and Gharehpetian, G., "Generation Expansion Planning and Generation unit Location Based on IGA and AHP", Energy Engineering & Management (JEM), Vol. 3, No.2, pp. 2-13, 2013.

[2] Amini, A., Falaghi, H. and ramezani, M., "Electric Load Dispatch Among Power Plants in order to Reduce Fuel Cost and Environmental Pollution", Energy Engineering & Management (JEM), Vol. 3, No.1, pp. 2-15, 2013.

[3] Gil M., Dueñas, P. and Reneses, J., "Electricity and Natural Gas Interdependency: Comparison of Two Methodologies for Coupling Large Market Models Within the European Regulatory Framework", IEEE Transactions on Power Systems, Vol. 31, No. 1, pp: 361-369, 2015.

[4] Rubio, R., Ojeda-Esteybar, D., Ano, O. and Vargas, A., "Integrated natural gas and electricity market: A survey of the state of the art in operation planning and market issues", IEEE/PES Transmission and Distribution Conference and Exposition: Latin America, pp: 1-8, 2008.

[5] Yu, W., Song, S., Li, Y., Min, Y., Huang, W., Wen, K. and Gong J. "Gas supply reliability assessment of natural gas transmission pipeline systems", Energy, Vol.12, No.1, pp: 162: 853-70, 2018.

[6] Bao, M., Ding, Y., Singh, C. and Shao, C. "A Multi-State Model for Reliability Assessment of Integrated Gas and Power Systems Utilizing Universal Generating Function Techniques", IEEE Trans Smart Grid, Vol.10, No.6, pp: 6271-6283, 2019.

[7] Deane, J. P., Ciaráin M.O. and Gallachóir, BP Ó., "An integrated gas and electricity model of the EU energy system to examine supply interruptions", Applied Energy, Vol. 193, No. 1 pp: 479-490, 2017.

[8] Unsihuay, C., Marangon Lima, JW. and Zambroni, De Souza, AC., "Modeling the integrated natural gas and electricity optimal power flow", IEEE Power Engineering Society General Meeting, pp: 1-7, 2007.

[9] He, C., Zhang, X., Liu T. and WU, L., "Distributionally robust scheduling of integrated gas-electricity systems with demand response", IEEE Transactions on Power Systems, Vol. 34, No. 5, pp: 3791-3803, 2019.

[10] Chen, S., Wei, Z., Sun, G., Cheung, K.W. and Sun Y., "Multi-linear probabilistic energy flow analysis of integrated electrical and natural-gas systems", IEEE Transactions on Power Systems, Vol. 32, No. 3 pp: 1970-1979, 2016.

[11] Massrur HR., Niknam T. and Aghaei J., "Fast decomposed energy flow in large-scale integrated electricity–gas–heat energy systems", IEEE Trans on Sustainable Energy, Vol. 9, No. 4, pp: 1565-1577, 2018.

[12] Gao, H. and Li, Z., "A Benders Decomposition Based Algorithm for Steady-State Dispatch Problem in an Integrated Electricity-Gas System", IEEE Transactions on Power Systems, in press, 2021.

[13] Badakhshan, S., Hajibandeh, H. and Shafie-khah, M., "Impact of solar energy on the integrated operation of electricity-gas grids", Energy, Vol. 183, No. 1, pp: 844-853, 2019.

[14] Chen, R., Wang, J. and Sun, H., "Clearing and pricing for coordinated gas and electricity day-ahead markets considering wind power uncertainty", IEEE Transactions on Power Systems, Vol. 33, No. 3, pp:2496-2508, 2017.

[15] Ghaffarpour, R., moradi, S. and ranjbar, A., "Optimal Planning of Energy Hub for Joint Operation of Electricity and Gas Systems Considering Reliability", Energy Engineering & Management (JEM), Vol. 7, No. 3, pp: 2-19, 2017.

[16] Cao, Z., Wang, J., Zhao, Q., Han, Y. and Li, Y, "Decarbonization Scheduling Strategy Optimization for Electricity-Gas System Considering Electric Vehicles and Refined Operation Model of Power-to-Gas", IEEE Access, Vol. 9, No.1, pp: 5716-5733, 2021.

[17] Badakhshan, S., Ehsan, M., Shahidehpour, M., Hajibandeh, N., Shafie-Khah, M. and Catalão, J. P, "Security-constrained unit commitment with natural gas pipeline transient constraints", IEEE Transactions on Smart Grid, Vol. 11, No. 1, pp: 118-128, 2019.

[18] Zhang, X., Shahidehpour, M., Alabdulwahab, A. and Abusorrah, A., "Hourly electricity demand response in the stochastic day-ahead scheduling of coordinated electricity and natural gas networks", IEEE Transactions on Power Systems, Vol. 31 No. 1, pp: 592-601, 2015

[19] Zhang, X., Che, L., Shahidehpour, M., Alabdulwahab, A. and Abusorrah, A., "Electricity-natural gas operation planning with hourly demand response for deployment of flexible ramp", IEEE Transactions on Sustainable Energy, Vol. 7, No. 3, pp:996-1004, 2016.

[20] Rose, D., Schmidt, M., Steinbach, M.C. and Willert, B.M., "Computational optimization of gas compressor stations: MINLP models versus continuous reformulations", Mathematical Methods of Operations Research, Vol. 83, No. 3, pp: 409-444, 2016.

[21] Hennings, F., "Benefits and limitations of simplified transient gas flow formulations", In Operations Research Proceedings, Springer, Cham, pp: 231-237, 2017.

[22] Sharifzadeh, H. and Amjady, N., "Stochastic security-constrained optimal power flow incorporating preventive and corrective actions", Vol. 26, No. 11, pp: 2337-2352, 2016.

[23] Koch, T., Hiller, B., Pfetsch, M.E. and Schewe, L. eds., Evaluating gas network capacities, Society for Industrial and Applied Mathematics, 2015.

[24]